Inorganic Chemistry
Article

Inorg. Chem. **2011**, *50*, 463–470 **463**
DOI: 10.1021/ic100958r

Redox, Spectroscopic, and Photophysical Properties of Ru−Pt Mixed-Metal Complexes Incorporating 4,7-Diphenyl-1,10-phenanthroline as Efficient DNA Binding and Photocleaving Agents

Samantha L. H. Higgins,[†] Travis A. White,[†] Brenda S. J. Winkel,[‡] and Karen J. Brewer*[,†]

[†]*Department of Chemistry and* [‡]*Department of Biological Sciences, Virginia Polytechnic Institute and State University, Blacksburg, Virginia 24061-0212, United States*

Received May 13, 2010

The redox, spectroscopic, and photophysical properties as well as DNA interactions of the new bimetallic complexes $[(Ph_2phen)_2Ru(BL)PtCl_2]^{2+}$ (Ph_2phen = 4,7-diphenyl-1,10-phenanthroline, and BL (bridging ligand) = dpp = 2,3-bis(2-pyridyl)pyrazine, or dpq = 2,3-bis(2-pyridyl)quinoxaline) were investigated. These Ru-polyazine chromophores with Ph_2phen TLs (terminal ligands) and polyazine BLs are efficient light absorbers. The $[(Ph_2phen)_2Ru(BL)PtCl_2]^{2+}$ complexes display reversible $Ru^{II/III}$ oxidations at 1.57 (dpp) and 1.58 (dpq) V vs SCE (saturated calomel electrode) with an irreversible $Pt^{II/IV}$ oxidation occurring prior at 1.47 V vs SCE. Four, reversible ligand reductions occur at −0.50 $dpp^{0/-}$, −1.06 $dpp^{-/2-}$, −1.37 $Ph_2phen^{0/-}$, and −1.56 V vs SCE $Ph_2phen^{0/-}$. For the $[(Ph_2phen)_2Ru(dpq)PtCl_2]^{2+}$ complex, the first two reductions shift to more positive potentials at −0.23 and −0.96 V vs SCE. The electronic absorption spectroscopy is dominated in the UV region by $\pi\rightarrow\pi^*$ ligand transitions and in the visible region by metal-to-ligand charge transfer (MLCT) transitions at 517 nm for $[(Ph_2phen)_2Ru(dpp)PtCl_2]^{2+}$ and 600 nm for $[(Ph_2phen)_2Ru(dpq)PtCl_2]^{2+}$. Emission spectroscopy shows that upon attaching Pt to the Ru monometallic precursor the λ_{max}^{em} shifts from 664 nm for $[(Ph_2phen)_2Ru(dpp)]^{2+}$ to 740 nm for $[(Ph_2phen)_2Ru(dpp)PtCl_2]^{2+}$. The *cis*-$Pt^{II}Cl_2$ bioactive site offers the potential of targeting DNA by covalently binding the mixed-metal complex to DNA bases. The multifunctional interactions with DNA were assayed using both linear and circular plasmid pUC18 DNA gel shift assays. Both title complexes can bind to and photocleave DNA with dramatically enhanced efficiency relative to previously reported systems. The impact of the Ph_2phen TL on photophysics and bioreactivity is somewhat surprising given the Ru→BL charge transfer (CT) nature of the photoreactive state in the complexes.

Introduction

The metal-based compound cisplatin, *cis*-$[PtCl_2(NH_3)_2]$, is one of the most effective anticancer agents developed to date.[1−4] The biological activity of cisplatin arises from its ability to bind covalently to DNA, inhibit transcription and replication and ultimately cause cell death or apoptosis. However, significant side effects, tumor acquired resistance, and lack of water solubility has resulted in the development of cisplatin analogues and other transition metal-based complexes for cancer treatment.[5−7]

Ruthenium-based complexes have been suggested as another class of anticancer agents.[8−10] Ruthenium(II) polyazine complexes are also candidates for use in PDT (photodynamic therapy) because of their ability to absorb visible light, utilize tunable properties, and associate with DNA. The $[Ru(Ph_2phen)_3]^{2+}$ (Ph_2phen = 4,7-diphenyl-1,10-phenanthroline) complex shows more efficient DNA photocleavage than the prototypical $[Ru(bpy)_3]^{2+}$ (bpy = 2,2′-bipyridine), presumably because of a longer lived metal-to-ligand charge transfer excited state ^{3}MLCT with higher $^1O_2$ yields.[11−15] Although many Ru-polyazine LAs (light absorbers) can photocleave

*To whom correspondence should be addressed. E-mail: kbrewer@vt.edu.

(1) Sherman, S. E.; Gibson, D.; Wang, A. H. J.; Lippard, S. J. *J. Am. Chem. Soc.* **1988**, *110*, 7368.
(2) Abu-Surrah, A. S.; Kettunen, M. *Curr. Med. Chem.* **2006**, *13*(11), 1337–1357.
(3) Jung, Y. W.; Lippard, S. J. *Chem. Rev.* **2007**, *107*(5), 1387–1407.
(4) Sherman, S. E.; Lippard, S. J. *Chem. Rev.* **1987**, *87*, 1153–1163.
(5) van Zutphen, S.; Reedijk, J. *Coord. Chem. Rev.* **2005**, *249*(24), 2845–2853.
(6) Clarke, M. J. *Coord. Chem. Rev.* **2003**, *236*, 209–233.
(7) Jakupec, M. A.; Galanski, M.; Arion, V. B.; Hartinger, C. G.; Keppler, B. K. *Dalton Trans.* **2008**, 183–194.
(8) Clarke, M. J.; Sadler, P. J. *Metallopharmaceuticals.*, 1st ed.; Springer: New York, 1999.
(9) Richards, A. D.; Rodger, A. *Chem. Soc. Rev.* **2007**, *36*(3), 471–483.
(10) Hannon, M. *Chem. Soc. Rev.* **2007**, *36*, 280–295.
(11) Barton, J. K.; Basile, L. A.; Danishefsky, A.; Alexandrescu, A. *Proc. Natl. Acad. Sci. U.S.A.* **1984**, *81*, 1961–1965.
(12) Watts, R. J.; Crosby, G. A. *J. Am. Chem. Soc.* **1971**, *93*, 3184–3188.
(13) Watts, R. J.; Crosby, G. A. *J. Am. Chem. Soc.* **1972**, *94*, 2606–2614.
(14) Demas, J. N.; Harris, E. W.; McBride, R. P. *J. Am. Chem. Soc.* **1977**, *99*(11), 3547–3551.
(15) Kumar, C. V.; Barton, J. K.; Turro, N. J. *J. Am. Chem. Soc.* **1985**, *107*, 5518–5523.

Published on Web 12/14/2010

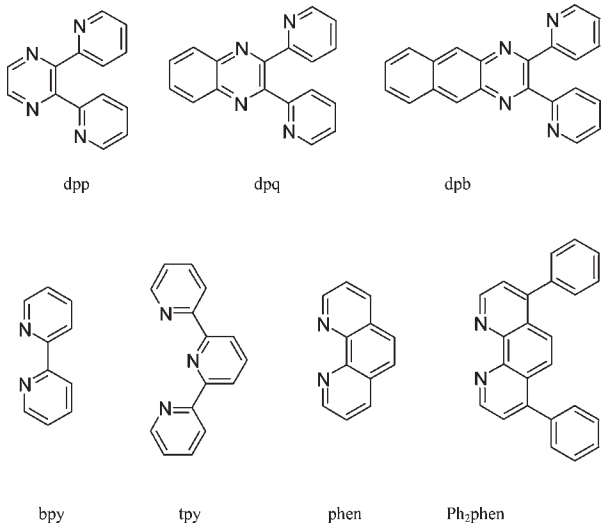

Figure 1. Structure of bridging ligands, dpp = 2,3-bis(2-pyridyl)pyrazine, dpq = 2,3-bis(2-pyridyl)quinoxaline, and dpb = 2,3-bis(2-pyridyl)benzoquinoxaline and terminal ligands bpy = 2,2′-bipyridine, tpy = 2,2′:6′2″-terpyridine, phen = 1,10-phenanthroline, and Ph_2phen = 4,7-diphenyl-1,10-phenanthroline.

DNA, the effective delivery of these compounds to their DNA targets inside the cell is essential to their successful application as PDT drugs.

The development of an emerging group of Ru−Pt supramolecular complexes could address targeted PDT and improve optical excitation into the therapeutic window.[16−19] Typical Ru−Pt bimetallic complexes couple the Ru LA directly to a Pt site, which impacts the photophysical properties of the systems.[20,21] The further development of an emerging group of Ru−Pt supramolecular complexes could address the restrictions of Pt-based complexes and provide a target for metal-based PDT agents, while maintaining efficient DNA binding and photocleaving properties.

Ru−Pt mixed-metal polyazine complexes have many properties that make them interesting as DNA targeting and modification agents. The complexes $[(bpy)_2Ru(BL)PtCl_2]^{2+}$ (BL = dpq and dpb) have been reported to more effectively reduce the electrophoretic migration of DNA in agarose gels compared to cisplatin as a result of Pt-centered covalent binding to DNA.[18] In addition, the positive charge of the bimetallic complex results in increased water solubility and enhanced electrostatic interactions of the Ru−Pt systems with the polyanionic DNA structure relative to cisplatin. Bimetallic complexes $[(tpy)RuCl(BL)PtCl_2]^{1+}$ (BL = dpp, dpq, and dpb, Figure 1) have shown avid binding to plasmid DNA, with $[(tpy)RuCl(dpp)PtCl_2]^{1+}$ being the first mixed-metal system shown to inhibit bacterial growth.[19] Though Ru−Pt bimetallic complexes have shown binding with DNA, photocleavage is typically not observed because of the relatively short-lived ^{3}MLCT excited states of these directly coupled systems. Our group has described the Ru−Pt tetrametallic complex, $[\{(bpy)_2Ru(dpp)\}_2Ru(dpp)PtCl_2](PF_6)_6$, with an intervening $Ru^{II}(BL)_3$ unit that covalently binds to DNA through Pt and upon exposure to visible light is able to cleave DNA through the terminal metal Ru→BL ^{3}MLCT excited state.[18] Herman and co-workers recently reported a Ru(III)/Pt(II) trimetallic complex, $Na_2\{$*trans, cis, trans*-$[Ru^{III}Cl_4$(S-DMSO)(μ-pyrazine)$]_2Pt^{II}Cl_2\}$ (AH-197), coupling both NAMI-A (NAMI-A = [*trans*-tetrachloro(1*H*-imidazole)(S-dimethylsulfoxide)ruthenate(III)]) and cisplatin-like subunits, that showed enhanced DNA binding and intermediate cytotoxicity in comparison to cisplatin and indazolium *trans*-[tetrachlorobis(1*H*-indazole)-ruthenate(III)], (KP1019).[22] Sakai and co-workers reported visible-light-induced double strand scission of DNA under air saturated conditions with $[Ru(bpy)_2(m$-bpy-$(CONH-(CH_2)_3-NH_2)_2\}PtCl_2](PF_6)_2$; however, photocleavage studies under deoxygenated conditions were not completed.[23]

Reported herein is the incorporation of the light absorbers, $[(Ph_2phen)_2Ru(dpp)]^{2+}$ and $[(Ph_2phen)_2Ru(dpq)]^{2+}$, into a Ru−Pt supramolecular complex to develop a general bimetallic structural motif that binds to and photocleaves DNA. The assay of the basic chemical, photophysical, and photoreactivity properties of these new Ru−Pt systems is reported.

Experimental Details

Materials. All reagents were used as received unless otherwise noted. $RuCl_3 \cdot 3H_2O$, 4,7-diphenyl-1,10-phenanthroline, and 1,3-diphenylisobenzofuran (DPBF) were purchased from Alfa Aesar. The bridging ligand, 2,3-bis(2-pyridyl)pyrazine, and KPF_6 were obtained from Aldrich. Spectral grade acetonitrile was obtained from Burdick and Jackson. Tetrabutylammonium hexafluorophosphate (Bu_4NPF_6) supporting electrolyte was purchased from Fluka. Sephadex LH-20 was purchased from GE Healthcare Biosciences Corporation. Circular pUC18 plasmid DNA was purchased from Bayou Biolabs. Lambda DNA/*Hin*dIII molecular weight marker was obtained from Promega. Linearized DNA was prepared from circular pUC18, using the *Hin*dIII restriction enzyme and NE Buffer 2 from New England BioLabs. Electrophoresis grade boric acid, agarose, and molecular biology grade glycerol were purchased from Fisher Scientific. The bridging ligand, dpq,[24] the monometallic precursor $[(Ph_2phen)_2Ru(dpp)]Cl_2$,[25] and the platinum starting material, $[PtCl_2(DMSO)_2]$,[26] were prepared according to previously published methods.

Preparation of $[(Ph_2phen)_2Ru(dpp)PtCl_2](PF_6)_2$. $[(Ph_2phen)_2Ru(dpp)PtCl_2](PF_6)_2$ was prepared by reacting the monometallic precursor with a labile Pt(II) reagent. $[(Ph_2phen)_2Ru(dpp)]Cl_2$ (0.50 g, 0.47 mmol) and $[PtCl_2(DMSO)_2]$ (1.0 g, 2.4 mmol) were heated at reflux in 25 mL of ethanol for 2 h in the dark. The reaction mixture was cooled to room temperature (RT), and the solid was collected by vacuum filtration. The solid was dissolved in a minimal amount of 2:1 ethanol/acetonitrile, filtered through a fine frit, and the filtrate was purified by LH-20 size exclusion chromatography using 2:1 ethanol/acetonitrile eluent. The first orange-red band was collected; solvent was removed under vacuum, and the complex was flash precipitated from dry acetone in diethyl ether, yield 75%. Metathesis to the PF_6^- salt involved

(16) Williams, R. L.; Toft, H. N.; Winkel, B.; Brewer, K. J. *Inorg. Chem.* **2003**, *42*, 4394–4400.
(17) Milkevitch, M.; Storrie, H.; Brauns, E.; Brewer, K. J.; Shirley, B. W. *Inorg. Chem.* **1997**, *36*, 4534–4538.
(18) Miao, R.; Mongelli, M. T.; Zigler, D. F.; Winkel, B. S.; Brewer, K. J. *Inorg. Chem.* **2006**, *45*, 10413–10415.
(19) Jain, A.; Winkel, B.; Brewer, K. J. *J. Inorg. Biochem.* **2007**, *101*, 1525–1528.
(20) Yam, V. W.-W.; Lee, V. W.-M.; Cheung, K.-K. *Organometallics* **1997**, *16*, 2833–2842.
(21) Masaoka, S.; Mukawa, Y.; Sakai, K. *Dalton Trans.* **2010**, *39*, 5868–5876.
(22) Herman, A.; Tanski, J. M.; Tibbetts, M. F.; Anderson, C. M. *Inorg. Chem.* **2008**, *47*, 274–280.
(23) Sakai, K.; Ozawa, H.; Yamada, H.; Tsubomura, T.; Hara, M.; Higuchi, A.; Hagac, M. A. *Dalton Trans.* **2006**, *27*, 3300–3305.
(24) Goodwin, H.; Lions, F. *J. Am. Chem. Soc.* **1959**, *81*, 6415–6422.
(25) Mongelli, M. T.; Brewer, K. J. *Inorg. Chem. Commun.* **2006**, *9*, 877–881.
(26) Price, J. H.; Williamson, A. N.; Schramm, R. F.; Wayland, B. B. *Inorg. Chem.* **1972**, *11*(6), 1280–1284.

dissolving $[(Ph_2phen)_2Ru(dpp)PtCl_2]Cl_2$ in a minimal amount of water and adding dropwise to a saturated aqueous solution of KPF_6. The solid was filtered, dried, and flash precipitated from acetonitrile in diethyl ether. The electrospray ionization mass spectrometry (ESI-MS) of $[(Ph_2phen)_2Ru(dpp)PtCl_2](PF_6)_2$ was consistent with the formulation, m/z: 1411 $[M - PF_6]^+$. The $^{195}Pt\{^1H\}$ NMR spectroscopy showed a single resonance, $\delta = -2170$ ppm.

Preparation of $[(Ph_2phen)_2Ru(dpq)](PF_6)_2$. $[(Ph_2phen)_2Ru(dpq)]Cl_2$ was synthesized by heating 25 mL of ethanol at reflux with $[(Ph_2phen)_2RuCl_2]$ (0.30 g, 3.6 mmol) and dpq (0.10 g, 3.5 mmol) for 3 h. The reaction mixture was cooled to RT, and the solvent was evaporated. The solid was purified by alumina chromatography using a 3:1 toluene:acetonitrile eluent, where the initial purple band was discarded. The orange-red band was collected and the solvent was removed under vacuum. The $[(Ph_2phen)_2Ru(dpq)]Cl_2$ was metathesized to the PF_6^- salt by adding the product dissolved in a minimal amount of water dropwise to a saturated aqueous solution of KPF_6. The solid was filtered and flash precipitated from acetonitrile upon addition to diethyl ether, with a yield of 65%. The ESI-MS of $[(Ph_2phen)_2Ru(dpq)](PF_6)_2$ showed m/z: 1195 $[M - PF_6]^+$.

Preparation of $[(Ph_2phen)_2Ru(dpq)PtCl_2](PF_6)_2$. $[(Ph_2phen)_2Ru(dpq)PtCl_2](PF_6)_2$ was synthesized by substitution of dpq for dpp. The monometallic precursor $[(Ph_2phen)_2Ru(dpq)](PF_6)_2$ (0.20 g, 0.18 mmol) and $[PtCl_2(DMSO)_2]$ (0.38 g, 0.90 mmol) were heated at reflux in 25 mL of ethanol for 2 h in the dark. The purification and metathesis procedures were the same as the dpp analogue, yielding $[(Ph_2phen)_2Ru(dpq)PtCl_2](PF_6)_2$, 70%. The ESI-MS of $[(Ph_2phen)_2Ru(dpq)PtCl_2](PF_6)_2$ was consistent with the formulation, m/z: 1461 $[M - PF_6]^+$. The $^{195}Pt\{^1H\}$ NMR spectroscopy showed a single resonance, $\delta = -1970$ ppm.

ESI-Mass Spectrometry. ESI-Mass Spectrometry was performed by M-Scan Inc., West Chester, PA, on a Micromass Q-TOF API US instrument. The samples were dissolved in acetonitrile and infused directly into the instrument source.

NMR Spectroscopy. NMR spectroscopy was collected using a Bruker AVANCE 600 MHz NMR. The samples were dissolved in CD_3CN and spectra were collected at room temperature. ^{195}Pt NMR spectroscopy experiment was referenced to K_2PtCl_4 ($\delta = -1614$ ppm).[27]

Electrochemistry. The redox properties of the complexes were studied by cyclic voltammetry on an Epsilon potentiostat from Bioanalytical Systems. A three electrode system was used; a platinum working electrode, a platinum wire auxiliary electrode, and a silver wire pseudo reference electrode. The scan rate for all studies was 100 mV/s. Background scans of the solvent showed no oxidative or reductive couples prior to adding solid samples. Following electrochemical analysis, ferrocene was added as an internal standard, ($FeCp_2/FeCp_2^+ = 0.43$ V vs SCE).[28] Analyses used a 0.1 M Bu_4NPF_6/CH_3CN supporting electrolyte/solvent system.

Electronic Absorption Spectroscopy. Electronic absorption spectra were recorded using a Agilent 8453 diode array spectrophotometer with a 2 nm resolution. The data were collected using Burdick and Jackson UV-grade acetonitrile at room temperature in a 1 cm quartz cell. Solutions for determining the extinction coefficient were prepared gravimetrically and reported as an average of three measurements.

Emission Spectroscopy. The room temperature emission spectra were recorded in deoxygenated Burdick and Jackson UV-grade acetonitrile solution using a modified Photon Technology, Inc. QuantaMaster Model QM-200−45E. The system was modified to use a 150 W cooled xenon lamp excitation source, with emission collected at a right angle by a thermoelectrically cooled Hamamatsu 1527 photomultiplier tube operating in photon counting mode. Data were reported for both air saturated and deoxygenated solutions. The air saturated samples were used as prepared, and the samples were then deoxygenated using solvent saturated with ultra high purity argon with sonication for 10 min prior to data collection. Direct comparisons were made by collection with the sample instrumental settings at the same time. This allows for variations in lifetimes of 1 ns and emission yields of 2% to be accurately determined. For 77 K emission, the samples were prepared as 4:1 ethanol/methanol absorbance-matched solutions. The samples were referenced to $[Os(bpy)_3](PF_6)_2$ with $\Phi^{em} = 4.6 \times 10^{-3}$ in deoxygenated conditions.[29] The spectra were corrected for detector response using the manufacturer supplied correction file.

Excited State Lifetime Measurements. The excited state lifetime measurements were completed at room temperature and at 77 K. Measurements were collected on a Photon Technology, Inc. (PTI) PL2300 nitrogen laser equipped with a PL 201 continuously tunable dye laser as an excitation source (360−900 nm). A Hamamatsu R928 red-sensitive photomultiplier tube collected the time profile of the emission at right angles. The signal was displayed on a LeCroy 9361 Dual 300 MHz oscilloscope. The data were fitted to a single exponential function using the equation $Y = A + Be^{-x/c}$ where c is τ in seconds.

Singlet Oxygen Quantum Yield, Φ_{1O2}. Singlet oxygen quantum yields were determined by a previously established method measuring the emission quenching of DPBF (1,3-diphenylisobenzofuran) in the presence of singlet oxygen produced from the metal complexes to form the non-emissive *o*-dibenzoylbenzene.[30,31] The $[Ru(Ph_2phen)_3]Cl_2$, $[(Ph_2phen)_2Ru(dpp)PtCl_2]Cl_2$, and $[(Ph_2phen)_2Ru(dpq)PtCl_2]Cl_2$ samples were prepared by absorbance matching, $A_{500\ nm} = 0.08$ AU, with a $[DPBF]_f = 20\ \mu M$ in a 2 mL sample. Each sample was photolyzed using an Oriel 1000 W Xe arc lamp fitted with a narrow bandpass filter ($\lambda_{irr} = 460-540$ nm). The emission spectroscopy was recorded in air-saturated methanol using the same instrumentation for emission spectroscopy with the slit width for the excitation and emission monochromators set at 2 nm. The samples were excited at 408 nm and the emission of the DPBF, following varied times of photolysis, was observed at 480 nm. The Ru−Pt bimetallic Φ_{1O2} were determined by graphing $(I_0 - I_t)/I_0$ vs t (minutes) (where t is time, I_0 is the emission intensity at photolysis time = 0, and I_t is the emission intensity at photolysis time = t), and the data was fitted with a linear trend line, $(I_0 - I_t)/I_0 = m(t) + 0$. The slope was referenced to the standard $[Ru(Ph_2phen)_3]Cl_2$, with $\Phi_{1O2} = 0.97$ to calculate the Φ_{1O2} for both Ru−Pt bimetallic complexes.[30]

Covalent Binding to Linearized pUC18 DNA. Agarose gel electrophoresis was used to analyze covalent binding of the bimetallic complexes to linear pUC18 DNA. Master solutions of the metal complexes were prepared in double deionized water (ddH_2O). The concentrations were varied by preparing solutions of 5:1, 10:1, and 20:1 BP (base pairs) of pUC18 DNA to MC (metal complex) in 100 mM NaH_2PO_4 buffer (pH = 7.0). The samples were incubated for 1 h at 37 °C. A Tris-Boric Acid (TB) buffer solution was prepared with 45 mM Tris base and 45 mM boric acid (pH = 7.4). To assay covalent DNA binding, 10 μL of the sample solutions (0.1 μg of linear pUC18 DNA) were mixed with 2 μL of glycerine based loading dye and loaded into the wells of a 30 mL gel prepared with 0.8% w/w agarose and 20% w/w TB buffer. Electrophoresis was performed using Owl Separation Systems, Inc., Model B1A electrophoresis state set at 105 V for 1.5 h. The gels were stained for 30 min in 0.5 μg/mL

(27) Still, B. M.; Kumar, P. G. A.; Aldrich-Wright, J. R.; Price, W. S. *Chem. Soc. Rev.* **2007**, *36*, 665–686.

(28) Scott, R. A.; Lukehart, C. M. *Applications of Physical Methods to Inorganic and Bioinorganic Chemistry*; John Wiley & Sons, Ltd: New York, 2007.

(29) Caspar, J. V.; Kober, E. M.; Sullivan, B. P.; Meyer, T. J. *J. Am. Chem. Soc.* **1982**, *104*(2), 632–634.

(30) Garcia-Fresnadillo, D.; Gergiadou, Y.; Orellana, G.; Braun, A. M.; Oliveros, E. *Helv. Chim. Acta* **1996**, *79*, 1222–1238.

(31) Ding, H.-Y.; Wang, X.-S.; Song, L.-Q.; Chen, J.-R.; Yu, J.-H.; Chao-Li; Zhang, B.-W. *J. Photochem. Photobiol. A: Chem.* **2006**, *177*, 286–294.

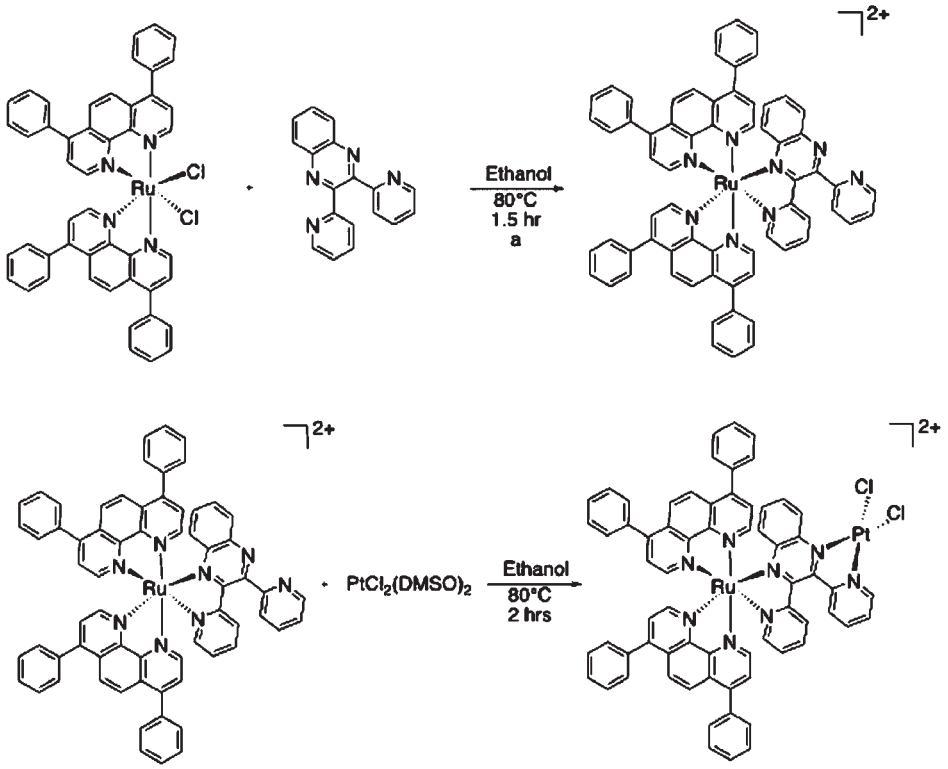

Figure 2. Synthetic scheme for $[(Ph_2phen)_2Ru(dpq)PtCl_2]Cl_2$. [a] Adapted from reference 26.

ethidium bromide (EtBr), destained for 15 min in ddH_2O, and visualized on a Fisher Scientific FBTI-88 transilluminator. Photographs were taken using an Olympus E-320 digital camera equipped with a Peca Products Inc. EtBr filter.

DNA Photocleavage Studies with Circular Plasmid pUC18 DNA. Agarose gel electrophoresis was also used to assay photocleavage of circular plasmid pUC18 DNA by the complexes. Metal complex/DNA solutions were prepared with ddH_2O and 100 mM NaH_2PO_4, forming a 20:1 BP/MC ratio. A LED array, consisting of eight thermostatted cells using 5 W Luxeon Royal Blue Star LEDs (λ_{max} = 455 nm, total average flux = $2.0 \pm 0.1 \times 10^{19}$ photons/min), was used for photolysis.[32] The 1 mL samples were photolyzed for 1 h under air saturated conditions or in the presence of a singlet oxygen quencher, sodium azide (0.1 M). The sodium azide samples were prepared by adding in the following order: sodium azide, buffer, DNA, water, and then MC. A freeze−pump−thaw (FPT) 20:1 BP/MC sample was prepared, six FPT cycles were completed, and the sample was photolyzed for 1 h. Identical samples were incubated at either RT or 37 °C in the dark for 1 h. Electrophoresis and imaging were completed as above.

Results and Discussion

Synthesis. The mixed-metal complexes were synthesized using a building block approach, which allows for ease of construction and characterization, Figure 2. The Ph_2phen terminal ligand was complexed to Ru to produce $[(Ph_2phen)_2RuCl_2]$, which, when bound to a bridging ligand and reacted with a *cis*-$Pt^{II}Cl_2$ moiety, produces the product $[(Ph_2phen)_2Ru(BL)PtCl_2](PF_6)_2$ (BL = dpp or dpq) in high yield. The monometallic and title bimetallic complexes were synthesized as chloride salts and metathesized to PF_6^- salts for characterization. The ESI mass spectral data for the $[(Ph_2phen)_2Ru(BL)PtCl_2](PF_6)_2$ complexes were consistent with their formulation, with a $[M - PF_6]^+$ peak at m/z = 1411 (BL = dpp) and 1461 (BL = dpq).

NMR Spectroscopy. ^{195}Pt NMR spectroscopy was used to analyze complexation of platinum to the monometallic precursor. The $[PtCl_2(DMSO)_2]$ starting material displays a ^{195}Pt resonance at −2980 ppm. For the $[(Ph_2phen)_2Ru(dpp)PtCl_2](PF_6)_2$ complex, a single resonance was observed at −2170 ppm, consistent with binding of Pt to the monometallic precursor. At −1970 ppm, a single resonance occurred, consistent with the formation of the $[(Ph_2phen)_2Ru(dpq)PtCl_2](PF_6)_2$ bimetallic complex with Pt bound to dpq. ^{195}Pt NMR showed no other detectable Pt containing materials in the bimetallic samples.

Electrochemistry. The electrochemistry of Ru-polyazine complexes typically shows reversible ruthenium-based oxidations followed by reversible one electron ligand-based reductions with the BL reductions occurring positive of the $TL^{0/-}$ couples. The electrochemical properties of the monometallic precursors and title bimetallic complexes were studied by cyclic voltammetry. The data are summarized in Table 1 and shown in Figure 3. The monometallic synthon, $[(Ph_2phen)_2Ru(dpp)](PF_6)_2$, displays a reversible $Ru^{II/III}$ oxidation at 1.40 V vs SCE, and $dpp^{0/-}$, $Ph_2phen^{0/-}$, $Ph_2phen^{0/-}$ reductions at −1.02 V, −1.37 V, and −1.56 V vs SCE consistent with previous reports.[25] Upon changing the BL from dpp to dpq, the $Ru^{II/III}$ reversible oxidation and the two $TL^{0/-}$ reversible reductions are largely unperturbed, while the $BL^{0/-}$ reversible reduction shifts anodically to −0.75 V vs SCE for the dpq complex. This establishes the BL as the site of the localization of the lowest unoccupied molecular orbital (LUMO) in these complexes, a point of question in our previous reports.[17,25] Platination of the complexes stabilizes the BL(π^*) orbital giving $BL^{0/-}$ and $BL^{-/2-}$

(32) Prussin, A. J.; Zigler, D. F.; Jain, A.; Brown, J. R.; Winkel, B. S.; Brewer, K. J. *J. Inorg. Biochem.* **2008**, *102*, 731–739.

Table 1. Electrochemical Data for $[(Ph_2phen)_2Ru(BL)](PF_6)_2$ and $[(Ph_2phen)_2Ru(BL)PtCl_2](PF_6)_2$

complex[a]	$E_{1/2}^{ox}$ (V)[b]	$E_{1/2}^{red}$ (V)[b]
$[(Ph_2phen)_2Ru(dpp)](PF_6)_2$[c]	+1.40 $Ru^{II/III}$	−1.02 $dpp^{0/-}$
		−1.37 $Ph_2phen^{0/-}$
		−1.56 $Ph_2phen^{0/-}$
$[(Ph_2phen)_2Ru(dpp)PtCl_2](PF_6)_2$	+1.57 $Ru^{II/III}$	−0.50 $dpp^{0/-}$
	+1.47 $Pt^{II/IV}$[d]	−1.06 $dpp^{-/2-}$
		−1.37 $Ph_2phen^{0/-}$
		−1.56 $Ph_2phen^{0/-}$
$[(Ph_2phen)_2Ru(dpq)](PF_6)_2$	+1.41 $Ru^{II/III}$	−0.75 $dpq^{0/-}$
		−1.37 $Ph_2phen^{0/-}$
		−1.56 $Ph_2phen^{0/-}$
$[(Ph_2phen)_2Ru(dpq)PtCl_2](PF_6)_2$	+1.58 $Ru^{II/III}$	−0.23 $dpq^{0/-}$
	+1.47 $Pt^{II/IV}$[d]	−0.99 $dpq^{-/2-}$
		−1.37 $Ph_2phen^{0/-}$
		−1.56 $Ph_2phen^{0/-}$

[a] Ph_2phen = 4,7-diphenyl-1,10-phenanthroline, dpp = 2,3-bis(2-pyridyl)pyrazine, and dpq = 2,3-bis(2-pyridyl)quinoxaline. [b] Recorded in 0.1 M Bu_4NPF_6 CH_3CN, with potential reported in V vs SCE, using a Ag wire pseudo reference electrode and ferrocene internal standard ($FeCp_2/FeCp_2^+$ = 0.43 V vs SCE).[28] [c] Redox potentials consistent with those in ref 27. [d] E_p^a.

couples prior to the $TL^{0/-}$ couples.[20] A small shift to positive potential is seen for the $Ru^{II/III}$ couple upon platination, now at +1.57 V (dpp) and +1.58 V (dpq). Prior to the $Ru^{II/III}$ oxidation an irreversible $Pt^{II/IV}$ oxidation occurs as a shoulder at approximately +1.47 V vs SCE.

The redox properties of the monometallic and bimetallic complexes help to understand the orbital energetics. For all four of the complexes, the electrochemistry predicts a Ru(dπ)-based highest occupied molecular orbital (HOMO) and a BL(π*)-based LUMO. This further predicts a Ru(dπ)→BL(π*) MLCT lowest lying excited state. The lower energy dpq(π*) orbital results in a reduced HOMO−LUMO energy gap, predicting a lower energy MLCT excited state compared to the dpp analogues.

Electronic Absorption Spectroscopy. The electronic absorption spectroscopy of the monometallic precursors and the title bimetallic complexes are shown in Figure 4. The complexes are efficient light absorbers throughout the UV and visible regions. The UV region is dominated by IL (IL = intraligand) Ph_2phen $\pi\rightarrow\pi^*$ transitions at 274 nm (ε = ca. 90,000 M^{-1} cm^{-1}), and the dpp $\pi\rightarrow\pi^*$ transitions at 310 nm (ε = ca. 35,000 M^{-1} cm^{-1}) or the dpq $\pi\rightarrow\pi^*$ transition at 320 nm (ε = ca. 34,000 M^{-1} cm^{-1}). For these systems the dpq $\pi\rightarrow\pi^*$ transitions are lower energy than those of dpp and those of Ph_2phen. The visible region of the spectrum is dominated by ^{1}MLCT transitions for each acceptor ligand. The Ru(dπ)→Ph_2phen(π*) CT transitions occurring at 424 nm (ε = approximately 18,000 M^{-1} cm^{-1}) are relatively unchanged for the series of complexes. The Ru(dπ)→dpp(π*) CT band red shifts from 474 nm (ε = 15,000 M^{-1} cm^{-1}) to 520 nm (ε = 11,400 M^{-1} cm^{-1}) upon platination of the monometallic complex because of stabilized BL(π*) acceptor orbitals. The monometallic Ru(dπ)→dpq(π*) CT transition at 522 nm (ε = 11,200 M^{-1} cm^{-1}) shifts to lower energy at 600 nm (ε = 9,800 M^{-1} cm^{-1}) for the bimetallic complex. The Ph_2phen TL and dpp or dpq BL provides systems with enhanced spectral coverage throughout the UV and visible, without the typical drop in the 350−450 nm region for bpy and phen systems.[22,27] By calculating the $\Delta E_{1/2}$ between the $Ru^{II/III}$ oxidation and the $BL^{0/-}$ reduction for the bpy, phen, and

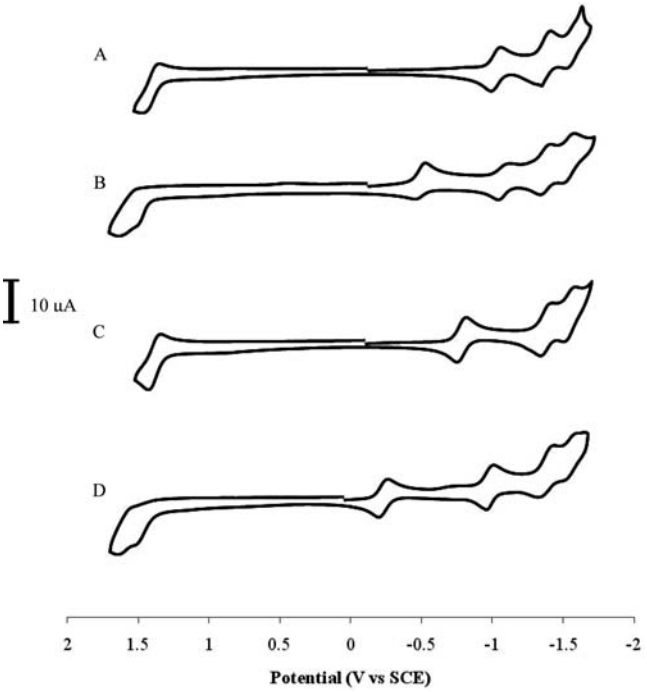

Figure 3. Cyclic voltammograms of $[(Ph_2phen)_2Ru(dpp)](PF_6)_2$ (A), $[(Ph_2phen)_2Ru(dpp)PtCl_2](PF_6)_2$ (B), $[(Ph_2phen)_2Ru(dpq)](PF_6)_2$ (C), and $[(Ph_2phen)_2Ru(dpq)PtCl_2](PF_6)_2$ (D), in 0.1 M Bu_4NPF_6 CH_3CN, reported vs SCE. (Ph_2phen = 4,7-diphenyl-1,10-phenanthroline, dpp = 2,3-bis(2-pyridyl)pyrazine, and dpq = 2,3-bis(2-pyridyl)quinoxaline).

Ph_2phen monometallic and bimetallic analogues, and comparing it to the E_{abs}, a clear correlation is evident, supporting similar spectroscopic and redox orbitals (E_{abs} = $0.94\Delta E_{1/2} + 0.37$, correlation = 0.95).[33,34]

Emission Spectroscopy. The Ru-polyazine monometallic complexes and the Ru−Pt dpp bridged bimetallic system display emission from their lowest lying Ru(dπ)→BL(π*) ^{3}MLCT excited state. Emission spectra are shown in Figure 3 and summarized in Table 2. Ru-based complexes are typically excited to their ^{1}MLCT excited state and undergo non-radiative intersystem crossing with unit efficiency to the lower energy ^{3}MLCT excited state from which the emission is derived. In general, monometallic complexes are more strongly emissive than the related bimetallic complexes because of the lower lying ^{3}MLCT states of the bimetallic complexes. The $[(Ph_2phen)_2Ru(dpp)](PF_6)_2$ monometallic complex displays an intense emission from the ^{3}MLCT state at RT in deoxygenated CH_3CN at λ_{max}^{em} = 664 nm ($\Phi^{em} = 3.5 \times 10^{-2}$, τ = 820 ns, $k_r = 4.3 \times 10^4$ s^{-1}, $k_{nr} = 1.2 \times 10^6$ s^{-1}), which narrows and shifts to 607 nm (τ = 5.4 μs) in 77 K, 4:1 EtOH/MeOH glass. The $[(Ph_2phen)_2Ru(dpq)](PF_6)_2$ monometallic complex has a red-shifted emission relative to the dpp system in RT deoxygenated CH_3CN at 758 nm ($\Phi^{em} = 1.1 \times 10^{-4}$, τ = 20 ns, $k_r = 5.5 \times 10^3$ s^{-1}, $k_{nr} = 5.0 \times 10^7$ s^{-1}) and displays an emission at 715 nm (τ = 1.7 μs) at 77 K in EtOH/MeOH glass. This red shift for the dpq complex is consistent with the spectroscopy and electrochemistry, which predicts a lower lying dpq(π*) acceptor orbital and a

(33) Rillema, D. P.; Allen, G.; Meyer, T. J.; Conrad, D. *Inorg. Chem.* **1983**, *22*, 1617–1622.
(34) Barigelletti, F.; Juris, A.; Balzani, V.; Belser, P.; Zelewsky, A. v. *Inorg. Chem.* **1987**, *26*, 4115–4119.

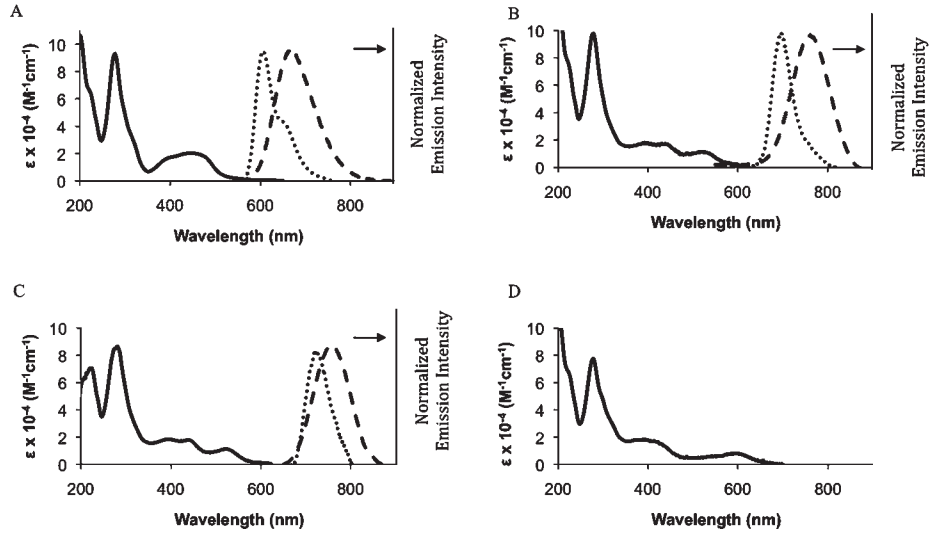

Figure 4. Electronic absorption and emission spectroscopy for $[(Ph_2phen)_2Ru(dpp)](PF_6)_2$ (A), $[(Ph_2phen)_2Ru(dpp)PtCl_2](PF_6)_2$ (B), $[(Ph_2phen)_2Ru(dpq)](PF_6)_2$ (C), and $[(Ph_2phen)_2Ru(dpq)PtCl_2](PF_6)_2$ (D). Electronic absorption in CH_3CN (solid line), RT emission spectroscopy in CH_3CN (dashed line), and 77 K emission in 4:1 EtOH/MeOH glass (dotted line). (Ph_2phen = 4,7-diphenyl-1,10-phenanthroline, dpp = 2,3-bis(2-pyridyl)pyrazine, and dpq = 2,3-bis(2-pyridyl)quinoxaline).

Table 2. Spectroscopic and Photophysical Data for $[(Ph_2phen)_2Ru(BL)](PF_6)_2$ and $[(Ph_2phen)_2Ru(BL)PtCl_2](PF_6)_2$, Where BL = dpp or dpq

complex[a]	λ_{max}^{abs} (nm)	λ_{max}^{em} (nm) RT	Φ^{em} RT Ar[b]	Φ^{em} RT atm[c]	τ(ns) RT Ar[d]	τ(ns) RT atm[e]	λ_{max}^{em} (nm) 77 K[f]	τ (μs) 77 K
$[(Ph_2phen)_2Ru(dpp)](PF_6)_2$	474	664	$3.5 \pm 0.2 \times 10^{-2}$	$1.5 \pm 0.1 \times 10^{-2}$	820 ± 20	386 ± 10	607	5.4
$[(Ph_2phen)_2Ru(dpp)PtCl_2](PF_6)_2$	517	740	$4.1 \pm 0.2 \times 10^{-4}$	$3.6 \pm 0.2 \times 10^{-4}$	44 ± 1	40 ± 1	694	2.3
$[(Ph_2phen)_2Ru(dpq)](PF_6)_2$	522	758	$1.1 \pm 0.06 \times 10^{-4}$	$9.6 \pm 0.5 \times 10^{-5}$	20 ± 1	18 ± 1	715	1.7
$[(Ph_2phen)_2Ru(dpq)PtCl_2](PF_6)_2$	600							

[a] Ph_2phen = 4,7-diphenyl-1,10-phenanthroline, dpp = 2,3-bis(2-pyridyl)pyrazine, and dpq = 2,3-bis(2-pyridyl)quinoxaline. [b] Deoxygenated with Ar, CH_3CN solution, referenced to $[Os(bpy)_3]^{2+}$, $\Phi^{em} = 4.6 \times 10^{-3}$. [c] Air saturated, CH_3CN solution, referenced to $[Os(bpy)_3]^{2+}$, $\Phi^{em} = 4.6 \times 10^{-3}$. [d] Deoxygenated with Ar, CH_3CN solution. [e] Air saturated, CH_3CN solution. [f] Collected in 4:1 ethanol/methanol glass at 77 K.

stabilized ^{3}MLCT state. The $[(Ph_2phen)_2Ru(dpp)PtCl_2](PF_6)_2$ complex emits at 740 nm ($\Phi^{em} = 4.1 \times 10^{-4}$, τ = 44 ns, $k_r = 9.3 \times 10^3\ s^{-1}$, $k_{nr} = 2.3 \times 10^7\ s^{-1}$) in RT deoxygenated CH_3CN and 694 nm (τ = 2.3 μs) at 77 K. Emission was not observed for $[(Ph_2phen)_2Ru(dpq)PtCl_2](PF_6)_2$ under our conditions, consistent with its most stabilized ^{3}MLCT excited state.

The change in the emission quantum yields of the complexes at RT under air saturated conditions was also studied to probe the ability of these chromophores to be quenched by molecular oxygen. The monometallic complex, $[(Ph_2phen)_2Ru(dpp)](PF_6)_2$ was readily quenched by molecular oxygen with a $\Phi^{em} = 1.5 \times 10^{-2}$ and τ = 386 ns in aerated solution vs $\Phi^{em} = 3.5 \times 10^{-2}$ and τ = 820 ns under deoxygenated conditions. The $[(Ph_2phen)_2Ru(dpp)PtCl_2](PF_6)_2$ and $[(Ph_2phen)_2Ru(dpq)](PF_6)_2$ complexes showed quenching of their RT emissions, but to a lesser extent with $\Phi^{em} = 3.6 \times 10^{-4}$ and τ = 40 ns and $\Phi^{em} = 9.6 \times 10^{-5}$ and τ = 18 ns under air saturated conditions vs $\Phi^{em} = 4.1 \times 10^{-4}$ and τ = 44 ns and $\Phi^{em} = 1.1 \times 10^{-4}$ and τ = 20 ns in deoxygenated conditions, respectively. These differences are small and predict a low quantum yield for singlet oxygen generation by these complexes. To further quantify the production of singlet oxygen, the singlet oxygen quantum yield was determined indirectly via the quenching of DPBF (1,3-diphenylisobenzofuran) emission. The $[Ru(Ph_2phen)_3]^{2+}$ complex was used as a standard reference, $\Phi_{1O2} = 0.97$, resulting in $\Phi_{1O2} = 0.067$ and 0.033 for $[(Ph_2phen)_2Ru(dpp)PtCl_2]Cl_2$ and $[(Ph_2phen)_2Ru(dpq)PtCl_2]Cl_2$, respectively. These quantum yields for singlet production are significantly smaller than classical Ru monometallic light absorbers likely because of the shorter excited state lifetime of these chromophores. This covalent coupling of Pt to these chromophores shifts the excitation wavelength to lower energy and provides for DNA binding so that singlet oxygen is generated in close proximity to the DNA target. The quenching of emission in the presence of molecular oxygen and the determination of the singlet oxygen quantum yield suggests these Ru−Pt complexes could function as DNA photocleavage agents via an oxygen-mediated pathway.

DNA Binding Analysis. The binding of the Ru−Pt bimetallic complexes to linear double-stranded plasmid DNA was compared to cisplatin and assayed by gel electrophoresis. The results of the DNA binding studies for cisplatin, $[(Ph_2phen)_2Ru(dpp)PtCl_2]Cl_2$ and $[(Ph_2phen)_2Ru(dpq)PtCl_2]Cl_2$ are shown in Figure 5A, 5B, and 5C, respectively. Each gel shows incubation of various ratios of base pairs (BP) to metal complex (MC) for 1 h at 37 °C. The *cis*-$Pt^{II}Cl_2$ site in cisplatin has been shown to covalently bind to DNA, and it has shown similar covalent binding in the Ru−Pt bimetallic complexes. When cisplatin or the title bimetallic complexes are bound to linear DNA, retardation of the migration of DNA through the gel is observed, as a result of a change in the mass, charge, and/or tertiary structure of the DNA molecule following metal binding. For both title complexes and cisplatin DNA migration increases as the BP/MC ratio decreases, consistent with covalent modification of DNA. The reduced emission of the EtBr dye in

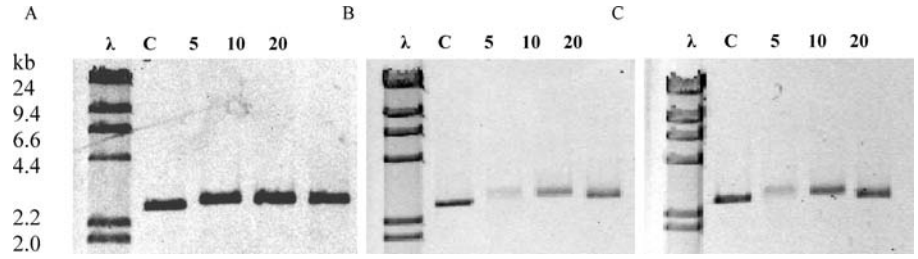

Figure 5. Gel electrophoresis studies of cisplatin (A), $[(Ph_2phen)_2Ru(dpp)PtCl_2]Cl_2$ (B), and $[(Ph_2phen)_2Ru(dpq)PtCl_2]Cl_2$ (C) with linear pUC18 DNA. The lanes for each gel correspond to (λ) lambda molecular weight marker (24, 9.4, 6.6, 4.4, 2.2, 2.0, and 0.56 kb), (**C**) linear pUC18 DNA control, (**5**) 5:1 BP/MC, (**10**) 10:1 BP/MC, and (**20**) 20:1 BP/MC.

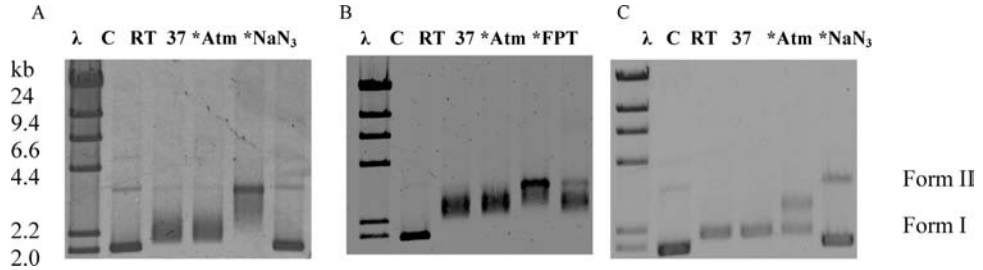

Figure 6. Electrophoretic mobility studies of the interaction of $[(Ph_2phen)_2Ru(dpp)PtCl_2]Cl_2$ (A and B) and $[(Ph_2phen)_2Ru(dpq)PtCl_2]Cl_2$ (C) with circular pUC18 plasmid DNA. The lanes for each gel correspond to (λ) lambda molecular weight marker (24, 9.4, 6.6, 4.4, 2.2, 2.0, and 0.56 kb), (**C**) linear pUC18 DNA control, (**RT**) 20:1 BP/MC ratio incubated at RT for 1 h, (**37**) 20:1 BP/MC incubated at 37 °C for 1 h, (***Atm**) 20:1 BP/MC ratio photolyzed for 1 h under air saturated conditions, (***NaN$_3$**) 20:1 BP/MC ratio photolyzed for 1 h in the presence of the singlet oxygen quencher, sodium azide (NaN_3), and (***FPT**) 20:1 BP/MC ratio photolyzed for 1 h following six FPT cycles.

lanes 5:1, 10:1, and 20:1 BP/MC relative to the uncomplexed control, **C**, for both Ru−Pt bimetallic complexes is characteristic of Ru−Pt mixed-metal systems and is not observed for cisplatin. This reduced emission is indicative of either energy transfer quenching of the EtBr excited state or inhibition of EtBr intercalation, upon metal binding.[17]

DNA Photocleavage Studies. The title bimetallic complexes were also assayed as DNA photocleavage agents. The metal complexes were combined with circular (uncleaved) supercoiled plasmid DNA and photolyzed under both air saturated and singlet oxygen quenching conditions. The samples were irradiated with a 5 W Luxeon Royal Blue Star LED (λ_{max} = 455 nm) array for 1 h and then analyzed by gel electrophoresis.[32] The pUC18 plasmid control indicates that most of the DNA is in the supercoiled (form I) state with a small amount of the open circular (form II) DNA. The gels show that the complexes bind to DNA at RT and 37 °C in the dark, lanes **RT** and **37**. Upon exposure to light for 1 h under air saturated conditions, $[(Ph_2phen)_2Ru(dpp)PtCl_2]Cl_2$ (lane ***Atm** in Figure 6A) and $[(Ph_2phen)_2Ru(dpq)PtCl_2]Cl_2$ (lane ***Atm** in Figure 6C) mediate the light activated cleavage of DNA. This process is O_2-dependent illustrated by the lack of DNA cleavage in the samples photolyzed in the presence of the singlet oxygen quencher, sodium azide (lanes ***NaN$_3$** in Figures 6A and 6C) and following six freeze pump thaw cycles (lane ***FPT** in Figure 6B). For the $[(Ph_2phen)_2Ru(dpp)PtCl_2]Cl_2$ complex a single strand cleavage to form open circular DNA is observed in air saturated conditions; however, in the presence of sodium azide DNA photocleavage and binding is inhibited. To further investigate this result, we studied the $[(Ph_2phen)_2Ru(dpp)PtCl_2]Cl_2$ DNA photocleavage properties after six freeze pump thaw cycles and photolysis for 1 h which shows photocleavage is inhibited after removal of O_2. The $[(Ph_2phen)_2Ru(dpq)PtCl_2]Cl_2$ system appears to linearize the DNA upon photolysis, consistent with cleavage of both DNA strands. This could result from the localized interaction of the Ru LA with the DNA target in a fixed location by covalent binding through the Pt site. This would allow multiple cleavage events because of multiple excitations, with the metal complex remaining at the site of the initial cleavage event. However, the specific DNA site that Pt binds is currently unknown at this time. These bimetallic complexes show enhanced photocleavage under lower light flux (LED vs arc lamp excitation) and with lower metal loading (20:1 vs 5:1 BP/MC ratios) than previously observed.[18,19,23] In fact, our typical deoxygenation conditions using argon do not sufficiently exclude oxygen to completely quench this pathway with the title complexes (data not shown). The Ph_2phen TL provides for enhanced ^{3}MLCT excited state lifetimes in this structural motif which should enhance photochemical reactions from this state such as singlet oxygen production. Localization of the Ru chromophore at the DNA via Pt binding should enhance reactivity of the $^1O_2$ produced with the DNA target. This photocleavage at low concentrations and light flux, and DNA targeting by covalent binding makes these systems of promise as potential PDT agents.

Conclusion

Two new bimetallic complexes, $[(Ph_2phen)_2Ru(BL)PtCl_2]^{2+}$ (BL = dpp or dpq), were synthesized by the building block method and were shown to have a number of interesting properties. The mixed-metal complexes display reversible $BL^{0/-}$, $BL^{-/2-}$, followed by two $TL^{0/-}$ reductions and oxidatively, $Pt^{II/IV}$ and $Ru^{II/III}$ oxidations. The electrochemistry predicts a Ru(dπ)-based HOMO and a BL(π*)-based LUMO. By changing the BL from dpp to dpq, the BL(π*) orbitals are stabilized providing a $BL^{0/-}$ reduction at more positive potential and reducing the HOMO−LUMO gap. The electronic

absorption spectroscopy is dominated by MLCT transitions in the visible region with the Ru→BL CT transition of the dpq analogue occurring at lower energy. Furthermore, by introducing the Ph_2phen terminal ligand, the electronic absorption spectroscopy shows reduced spectral gaps and increased absorptivity in the visible region compared to the bpy and phen analogues. The monometallic precursors and the $[(Ph_2phen)_2Ru(dpp)PtCl_2](PF_6)_2$ complex are emissive at RT and 77 K providing a probe to excited state dynamics, occurring from their lowest lying ^{3}MLCT excited state.

The title complexes $[(Ph_2phen)_2Ru(dpp)PtCl_2]Cl_2$ and $[(Ph_2phen)_2Ru(dpq)PtCl_2]Cl_2$ have shown the ability to covalently bind and photocleave DNA in marked contrast to previously studied dpp and dpq bridged systems. Gel electrophoretic studies with linear DNA show that the complexes covalently bind to the DNA through the *cis*-$PtCl_2$ bioactive site similar to cisplatin. Photolysis studies exciting the title complexes in the presence of plasmid DNA show marked photoreactivity as DNA photocleaving agents over previous Ru(II)−Pt(II) systems. The title bimetallic complexes photocleave DNA via an oxygen-dependent mechanism. The emission from the ^{3}MLCT excited states of these molecules is quenched by oxygen leading to the production of singlet oxygen with $\phi = 0.067$ and 0.033 for $[(Ph_2phen)_2Ru(dpp)PtCl_2]^{2+}$ and $[(Ph_2phen)_2Ru(dpq)PtCl_2]^{2+}$, respectively. Photocleavage is inhibited by freeze pump thaw degassing. Coupling the chromophore to DNA via the *cis*-$Pt^{II}Cl_2$ site directs the $^1O_2$ to the DNA target. Varying the BL impacts the nature and localization of the reactive ^{3}MLCT state and sterics around the Pt center which may modulate photoreactivity of these systems. Work is underway to study these systems and their bioactivity in further detail.

Acknowledgment. Acknowledgment is made to the NSF-CHE program (Grant CHE-0408445) for their generous partial support of this work. Acknowledgment is also made to Dr. Avijita Jain, Jing Wang, and Jessica Knoll for helpful discussions during this project.